IROS'95, Pittsburgh, PA, August 1995

Two-arm manipulation: What can we learn by studying humans?

Miloš Žefran, Vijay Kumar, Jaydev Desai and Ealan Henis[†]
GRASP Laboratory, University of Pennsylvania, Philadelphia, PA 19104-6228
[†]AT&T Bell Laboratories, Murray Hill, NJ 07974

Abstract

This paper addresses determination of trajectories and force distribution for cooperative manipulation with two arms through optimizing an integral cost function that depends on the actuator forces. We compare the calculated trajectories with the measurements on human subjects performing planar manipulation tasks. Our findings suggest that the trajectories and forces used by humans can be predicted by minimizing the integral of the rate of change of actuator torques over the trajectory. Good match is shown for a class of manipulation tasks in which the person-to-person variability is small. The theoretical foundation for computing the optimal solutions is briefly presented and the advantages of using such schemes for robotic systems are discussed.

1 Introduction

Planning of motions for two robots cooperatively manipulating an object occurs at three levels. First, given the initial configuration of the system and the goal position and orientation of the object, the trajectory of the object must be planned. Second, the appropriate joint trajectories must be chosen. Finally, forces must be distributed among the actuators to achieve the desired motion. Typically, kinematic and actuator redundancy occur in coordinated manipulation tasks. Therefore, all of the above problems involve choosing one solution among infinitely many possible solutions.

In most previous works, it is assumed that the trajectory of the object is prespecified. Hence, the focus has been on on-line control schemes for load sharing between the two robots [1, 2, 3, 4]. In these schemes, the actuator redundancy is resolved by locally minimizing a suitable cost function, which usually involves some measure of the internal forces. Alternatively, additional requirements can be specified for the manipulation task to eliminate the redundancy [5]. In contrast to these methods which achieve point-wise optimality, it is possible to obtain globally optimal solutions [6]. In this paper too, we pursue methods that will yield solutions for the trajectories while simultaneously resolving the kinematic and actuator redundancies.

It is instructive to observe how similar problems are solved by humans. Based on studies of single arm reaching in humans, Flash and Hogan [7, 8] have suggested that the central nervous system uses an optimality criterion to plan the trajectory. In medium speed, large amplitude, unconstrained planar motions for a single arm, the integral of the jerk along the trajectory is minimized. The *minimum-jerk* solution [8] depends only on the kinematics of the task. According to studies on coordinated manipulation with two arms by humans [9], the success of the minimum-jerk model in accounting for two-arm trajectories is limited. Kawato et al. [10, 11] proposed an alternative cost function for trajectory generation: the integral of the norm of the vector of derivatives of the actuator torques along the trajectory. This cost function (called *minimum torque-change* criterion), unlike the minimum-jerk criterion, takes into account the dynamics of the system.

Žefran et al. [6] investigated different cost functions for dual arm manipulation. The optimal movements of two two-link planar arms holding a small object were studied. They observed that the internal forces considerably affect the resulting trajectories. The minimum torque-change criterion yielded not only an optimal trajectory but also optimal internal forces.

In this paper, we study how humans coordinate their arms in two-arm manipulation tasks. We address all three levels of planning: a) trajectory planning; b) resolution of the kinematic redundancy; and c) determination of the force distribution. Motivated by the kinematic analysis of the experimental data [9] and by the findings from [6], we consider the minimum torque-change criterion. We first develop a dynamic model of the system and formulate the optimal control problem. We next present experimental observations of human two-arm manipulation. Finally, we compare the results predicted by the minimum torque-change model with the measured data. We conclude the paper with a discussion on the possible applications of our method.

2 Dynamics and optimal control

We study the case of two 3-R anthropomorphic manipulators in the horizontal plane holding an object as shown in Fig. 1. Each manipulator has 3 links and 3 actuated degrees of freedom (corresponding to the shoulder, elbow and wrist). The manipulators hold a rigid object. We assume that each grasp is rigid, hence all degrees of freedom of the system correspond to the degrees of freedom of the joints. Three parameters are needed to specify the position and the orientation of the object in the plane. The two manipulators and the object form a closed kinematic chain with a mobility of 3. Since the mobility is equal to the dimension of the task space, the system does not have any kinematic redundancy. However, because the number of actuators (6) exceeds the mobility, we have actuator redundancy.

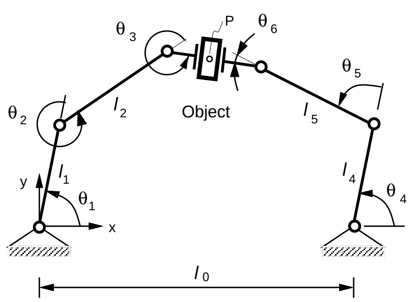

Figure 1: Two planar 3-R arms holding an object.

The dynamic equations of the closed chain formed by the two manipulators and the object can be derived using Lagrange multipliers:

$$\begin{aligned} I_1(\theta_1)\ddot{\theta}_1 + C_1(\theta_1, \dot{\theta}_1) + G_1(\theta_1) &= \tau_1 + \Gamma_1^T \lambda \\ I_2(\theta_2)\ddot{\theta}_2 + C_2(\theta_2, \dot{\theta}_2) + G_2(\theta_2) &= \tau_2 - \Gamma_2^T \lambda \end{aligned} \quad (1)$$

where θ_i, ω_i and τ_i $(i = 1, 2)$ are the 3×1 vectors containing joint angles, joint velocities and actuator forces of manipulator i, I_i is the 3×3 inertia matrix, C_i is the 3×1 vector of Coriolis and centrifugal forces, G_i is the 3×1 vector of gravity terms, Γ_i is the 3×3 Jacobian matrix, and λ is the 3×1 vector of Lagrange multipliers. The inertia of the object is distributed between the two arms and is incorporated into the I_i's.

For planar motions we can neglect the gravity terms. By eliminating the Lagrange multipliers from equations (1), a single equation is obtained:

$$\Gamma_1^{-T}\left[I_1\ddot{\theta}_1 + C_1 - \tau_1\right] = \Gamma_2^{-T}\left[I_2\ddot{\theta}_2 + C_2 - \tau_2\right]. \quad (2)$$

The actuator redundancy gives rise to a 3 dimensional space of internal forces. An internal force is a set of nonzero end effector forces (and moments) whose resultant is zero. Internal forces do not affect the motion of the object but they do perform isometric (dissipative) work. An example of an internal force in our system is a pair of pure forces such that the object (the link joining joints 3 and 6) is in compression or tension. We will refer to this axial component as F_a. For a given trajectory, resolving the actuator redundancy is equivalent to determining the internal force.

Motivated by previous studies of single-arm reaching tasks [8, 10], and by our own studies of two-arm manipulation [9, 6], we pursue the minimization of the integral of the norm of the actuator force change. The cost function is therefore

$$J = \frac{1}{2}\int_{t_0}^{t_f} \dot{\tau}^T \dot{\tau}\, dt \quad (3)$$

where $\tau = \left[\tau_1^T \; \tau_2^T\right]^T$ and $\dot{\tau}$ is the time derivative of τ (see Eq. 1).

We define the input vector to be

$$u = \dot{\tau}. \quad (4)$$

In order to write the dynamic equations of motion in standard state space notation, we define a state vector

$$x = \begin{bmatrix} x_1 \\ x_2 \\ x_3 \end{bmatrix} = \begin{bmatrix} p \\ \dot{p} \\ \tau \end{bmatrix}, \quad (5)$$

where p is a 3×1 vector consisting of the Cartesian coordinates of the center (P) of the object (handle) and its orientation, and $\dot{p}$ is the corresponding Cartesian velocity vector. The system dynamics in (2,4) can be rewritten as 12 first order differential equations:

$$\begin{bmatrix} \dot{x}_1 \\ \dot{x}_2 \\ \dot{x}_3 \end{bmatrix} = \begin{bmatrix} x_2 \\ A(x_1, x_2) + B(x_1)x_3 \\ 0 \end{bmatrix} + \begin{bmatrix} 0 \\ 0 \\ I \end{bmatrix} u \quad (6)$$

where $A(x_1, x_2)$ is a 3×3 matrix consisting of position and velocity dependent inertial terms and $B(x_1)$ is a 3×6 Jacobian matrix. This standard approach is described in greater detail in [2, 5].

Boundary conditions must be specified to solve the optimal control problem defined by (3,6). For each movement, we know the start and end positions. Further, the motion starts and ends with zero velocity and acceleration. Thus we have a total of 9 boundary conditions at each point. Since we have a 12-dimensional state space, we can specify 3 additional boundary conditions at each end [6]. For example, it may be meaningful to specify the internal forces at the beginning and the end of the maneuver.

The theoretical development for solving optimal control problems with state constraints is detailed in [12]. The optimal control problem with constraints is transformed into an unconstrained variational problem [13]. The integral form of the necessary conditions is solved by using finite-element methods. This leads to a robust and efficient solution procedure that typically converges in less than 10 iterations and runs around 60 seconds on a SGI Indigo.

3 Experimental results

Two-arm planar motions of human subjects were recorded using the three degree of freedom planar passive manipulandum shown in Figure 2. The apparatus consists of three links, connected by revolute joints. The third link is a handlebar that can rotate around its center. Three optical encoders mounted at each joint are used to record the manipulandum joint angles. Six axis force sensors are mounted underneath each handle, allowing measurement of the forces and torques exerted on the handles by the subject. The encoders and the force sensors are sampled at 150 Hz.

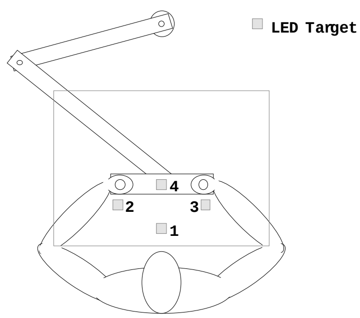

Figure 2: Experimental setup.

The subject is seated in front of a transparent Plexiglas plate and firmly grasps the two handles of the handlebar. The plate lies horizontally at the level of the subject's chin. Four target sets are mounted on the plate as shown in Fig. 2. Target 1 is 30cm in front of the subject's chest, Target 2 (Target 3) is displaced by 8.5cm forward and 15cm to the left (right) of Target 1, and Target 4 is displaced 19.5cm forward with respect to Target 1. Each target set consists of arrays of light emitting diodes (LED's) that can specify target positions and orientations. For detailed description of the experimental setup we refer the reader to [14, 9].

During the experiment, the room was darkened and a computer generated sequence of target configurations was displayed. The subjects were instructed to move the handlebar to the position and orientation specified by the lit targets at their preferred velocity. They were instructed to prevent slippage between the hands and the handles and to keep the elbows in the shoulder plane (so that a 1-1 correspondence between the manipulandum joint angles and the shoulder, elbow and wrist angles of the human arms was established). In all the experiments reported here, the subjects were instructed to keep the handlebar parallel to the frontal plane. Four subjects participated in the study: two right-handed, one left-handed and one ambidextrous.

Three types of motions were studied: a) motions parallel to the frontal plane ($2 \rightarrow 3$ and $3 \rightarrow 2$ in Fig. 2), b) motions in the sagittal plane ($1 \rightarrow 4$ and $4 \rightarrow 1$), and c) oblique motions ($1 \rightarrow 2$ and $1 \rightarrow 3$). Velocities and forces exerted on the handles by the left and the right arms were studied for each motion. All quantities are expressed in a coordinate frame located at the first target with the x-axis normal to the sagittal plane and pointing to the left and y-axis normal to the frontal plane and pointing forward. Only those components for which the prescribed amplitudes were nonzero are considered (e.g., the y components of motions parallel to the frontal plane are disregarded). These components will be referred to as "significant components". Because of limitations on space, we present only representative plots to give the reader a feel for the experiments and the data that was collected.

3.1 General observations

Velocity profiles: Some examples of normalized velocity profiles are shown in Fig. 3.a for different subjects. Only the significant components are shown. The velocity profiles are bell-shaped but the shape is not symmetric and the peak occurs on average at around 43% of the duration of motion. The rise to the peak is steeper than the fall to zero. Since the subjects did not have visual (end-point) feedback of the handle, it is not clear whether this effect can be attributed to a slowing down in order to achieve accurate positioning.

Force profiles: Some representative plots of the normalized significant components of the total force acting on the handle are shown in Fig. 3.b. The forces exerted on the object are roughly sinusoidal. The force profile for a particular subject is in general invariant with respect to the direction of motion, but it varies from person to person. In part, this difference can be attributed to different speeds at which different subjects performed the motions. At higher speeds (solid line in Fig. 3.b), the profile is roughly symmetric with the peak and the following valley having approximately the same duration and amplitude. At lower speeds, the peak was considerably sharper and higher than the valley.

Force distribution: Representative trajectories showing the axial component of the internal forces (F_a) are shown in Fig. 3.c. During motions with components in the x direction, the internal force component was nonzero. In other words, the distribution of forces between the two arms in the x direction is asymmetric. In contrast, the arm forces in the y direction were roughly equal.

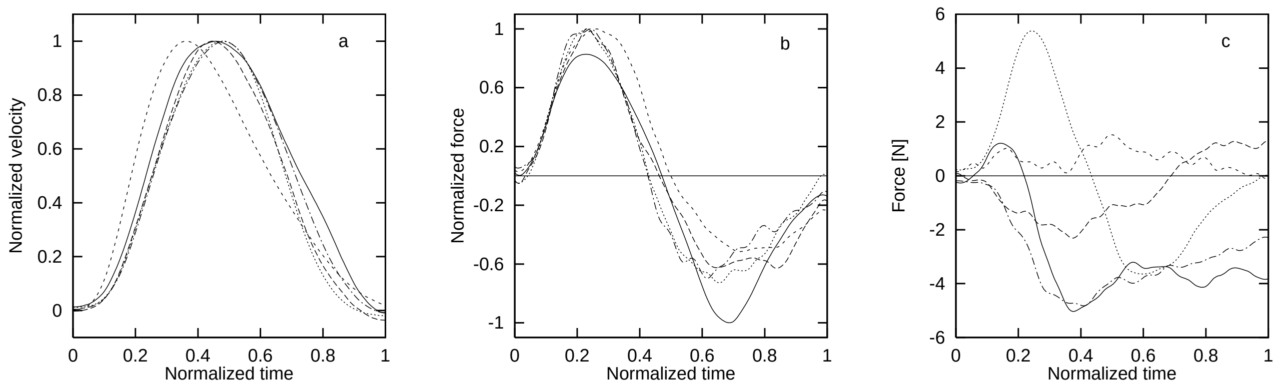

Figure 3: Sample plots of experimental data. a) Velocity. b) Total force acting on the object. c) Internal forces in the axial direction.

Remarks: Some of these observations are a natural consequence of the physics of the task and are not surprising. If the object is at rest at the beginning and at the end of motion, and the manipulation task is otherwise unconstrained, one can expect to see a bell-shaped velocity profile. The shape of the force profile is linked to the shape of the velocity profile because the total force is proportional to the acceleration. If the velocity is bell-shaped, the acceleration will be sinusoidal. The symmetry of the force distribution in the y direction can also be explained. The subjects did not exert large torsional moments at the handles which implies that it is not possible to exert internal forces with significant components in the y direction.

3.2 Motions in the sagittal plane

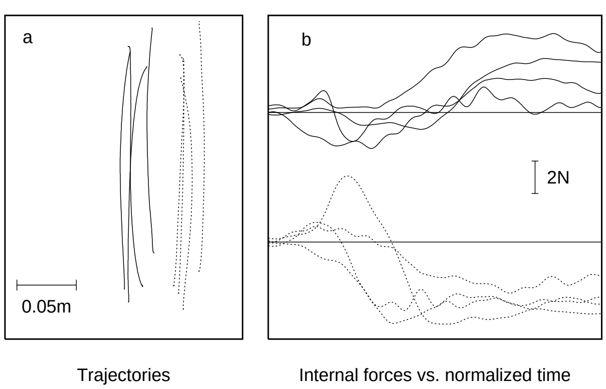

Figure 4: Motions in the sagittal plane. a) Trajectories for inward (solid) and outward (dotted) motions. b) Internal forces in the axial direction.

The Cartesian trajectories of the object for motions that are nominally in the sagittal plane are shown in Fig. 4.a. Inward trajectories are shown shifted to the left so that they can be compared to the outward trajectories. An interesting observation is that the trajectories are always curved. Further, outward trajectories ($1 \rightarrow 4$) curve in the opposite direction as inward trajectories ($4 \rightarrow 1$). For both, left and right-handed subjects, outward trajectories curve to the right while inward trajectories curve to the left. The corresponding internal forces (axial component only) are shown in Fig. 4.b. The axial component of the internal forces affects the forces in the x direction. When the subjects moved inwards, they exerted compressive forces (positive internal forces) on the handle, while on the way outwards the handle was in tension (negative internal forces). This appears to be due to the natural tendency of the arms to move closer together on the inward path, while on the way outward they tend to move apart. Analysis of the individual arm forces (not shown) indicates that in all cases the force exerted by the right arm had slightly higher amplitude (this was also true for the left-handed subject). Thus, on the inward motion, the arms compress the handle, and we can expect the trajectory to curve toward the left as corroborated by our observations. A similar argument can be made for the outward motion.

3.3 Other motions

A common characteristic of motions parallel to the frontal plane and oblique motions is that the amplitude of motion in the x direction is large. The only feature common to all these motions is the asymmetry of the forces in the x direction. Thus considerable internal forces (axial component) are always present (Fig. 3.c). The figure also indicates that the internal forces tend to start at zero, become compressive (positive) for a short period and are afterwards tensile (negative). This behavior can be observed for all movements with a significant component in the positive or negative x direction for left and right-handed subjects. Hence there is no ground to believe that the dominance of one arm over the other plays an important role. It is also interesting that the total force exerted on the object does not vary much from subject to subject, but the distribution of the force between the two arms varies greatly.

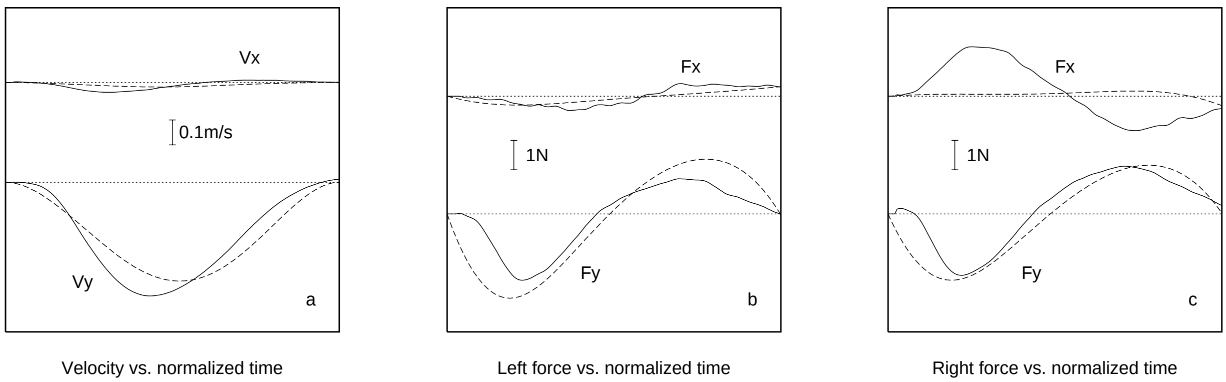

Figure 5: Comparison of the data (solid) with the predictions of the model (dashed): a) Velocities. b) Left-arm forces. c) Right-arm forces.

4 Optimal Forces and Trajectories Predicted by the Model

In this section we compare the optimal trajectories and force distribution predicted by the minimum torque-change model with the experimental observations. We chose a typical data set for a sagittal plane motion, $4 \rightarrow 1$. From this set we obtained the initial and final positions and forces of the left and the right arm for the optimization, and calculated the minimum torque-change trajectories. The physical dimensions of the arms for the optimization corresponded to the measurements of the subject. Dynamic parameters (mass and moments of inertia) of the human arm were calculated from the normalized anthropometric measurements reported by Winter [15].

Figure 5.a compares the velocity profiles predicted by the simulation (dashed) with the measured ones (solid). As expected, the simulation predicts that the velocity in the x direction will be close to 0. It is slightly curved because the measured initial and final points did not have the same x coordinate. The measured x velocity profile, on the other hand, considerably deviates from 0 because the measured trajectories are curved (Fig. 4.a). The predicted and observed y-velocity profiles have similar shapes, but there is also some discrepancy between the two: the measured trajectory reaches the valley at 43% of movement duration, while the computed attains its minimum at 53%. This disparity is also reflected in the amplitudes.

The comparison of the measured forces with those predicted by the simulation is shown in Figs. 5.b and 5.c. The agreement between the simulated and the measured forces is reasonable except for the force exerted by the right arm in the x direction where it is poor (Fig. 5.c). This discrepancy is due to an apparent dominance of the right arm over the left arm which was observed for both, left and right-handed subjects. The optimality criterion, on the other hand, does not incorporate such dominance. The discrepancy in the y force component is consistent with the differences of the velocity profiles in the y direction. The measured force profile exhibits a valley that is sharper than the ensuing peak. The two extrema (the valley and the peak) are also not symmetric about the midpoint. However, the optimization results are fairly symmetric.

The comparison of the computed and measured trajectories shows that the minimum torque-change model correctly predicts some features of the motion, at least when the effects causing asymmetric distribution of the load between the two arms are small. These features include the general shape of the trajectories, of the velocities and of the force distributions. While we have only presented results for one instance of motion, this set of data is typical of what we have observed with other subjects as well. On the other hand, there are important differences between the model predictions and the data. Most notably, the calculated velocity profile is quite symmetric while all measured velocity profiles are consistently asymmetric. At the force level, the major discrepancy is in the x component of the force. There is an apparent dominance of the right arm over the left arm, and neither our dynamic model nor the minimum torque-change criterion incorporates this effect. It is worth noting, however, that this dominance appears to be independent of whether the subject is left-handed, right-handed or ambidextrous. Finally, we have not attempted to compare the predicted results with the measurements for the other motions (motions with a significant component of velocity in the frontal plane), because of the variability of the force data across subjects.

5 Discussion

This paper addresses the optimization of trajectories and the distribution of forces in two cooperating arms in artificial and biological systems. We reported on experiments of human subjects performing planar manipulation tasks with two arms and attempted to explain the observed behavior with a model based on the minimum torque change criterion.

The observed trajectories were approximately straight lines with bell-shaped velocity profiles (along the x and y directions) and quite repeatable. The measured force distributions among the two arms were markedly asymmetric in the x direction and symmetric in the y direction. However, no consistent pattern could be observed among different subjects except in sagittal plane movements, where the right arm appeared to be dominant (regardless of whether the subjects were left or right-handed).

In the minimum torque change model, the objective function is the integral of the vector of derivatives of the actuator forces. Unlike other models, the minimum torque change criterion predicts the internal forces in addition to the trajectories of the system, and thus resolves indeterminacies at the trajectory, joint and actuator levels. It is also a dynamic smoothing principle that is directly applicable to robotics. With respect to our experiments with human subjects, the minimum torque change model seemed to reasonably predict the kinematic characteristics of the motions and the total force histories. However, it was unable to account for the observed dominance of the right arm over the left arm in sagittal plane motions. It is possible that a hierarchical bi-directional control scheme that operates at different planning levels, and is based on similar smoothing criteria can account for all the features of human two-arm manipulation movements by allowing to treat the two arms asymmetrically [11]. This is a direction for future investigation.

While single joint movements and single arm movements have been studied extensively, this work (see also [9]) is the first quantitative study of human manipulation using two arms. The objective of our experiments was to study and model human movements with the ultimate goal of improving our understanding of the control and planning problems in actively controlled over-constrained systems. It is worth noting that these studies are directly relevant to the design of human-machine interfaces, virtual reality systems and haptic interfaces. Our findings are also relevant to telerobotics where two-handed joysticks may afford better control of robotic systems, especially when the robotic systems consist of two or more arms.

Acknowledgment

This work has been supported by the NSF grants BCS 92-16691, MSS 91-521869, CISE/CDA 88-22719, and CISE/CDA 9022530 and the University of Pennsylvania Research Foundation. The first author was also supported by the Institute for Research in Cognitive Science, the University of Pennsylvania.

References

[1] Y. Zheng and J. Luh, "Optimal load distribution for two industrial robots handling a single object," in *IEEE International Conference on Robotics and Automation*, (Philadelphia, PA), Apr. 1988.

[2] X. Yun and V. Kumar, "An approach to simultaneous control of trajectory and interaction forces in dual-arm configurations," *IEEE Transactions of Robotics and Automation*, vol. 7, no. 5, 1991.

[3] D. Williams and O. Khatib, "The virtual linkage: a model for internal forces in multi-grasp manipulation," in *Proc. of 1993 IEEE Int. Conf. on Robotics and Automation*, (Atlanta, GA), 1993.

[4] K. Kreutz and A. Lokshin, "Load balance and closed chain multiple arm control," in *Proc. 1988 Amer. Control Conf.*, (Atlanta, GA), 1988.

[5] E. Paljug, X. Yun, and V. Kumar, "Control of rolling contacts in multi-arm manipulation," *IEEE Transactions on Robotics and Automation*, vol. 10, no. 4, 1994.

[6] M. Žefran, V. Kumar, and X. Yun, "Optimal trajectories and force distribution for cooperating arms," in *Proc. of 1994 IEEE Int. Conf. on Robotics and Automation*, (San Diego, CA), 1994.

[7] N. Hogan, "An organizing principle for a class of voluntary movements," *The Journal of Neuroscience*, vol. 4, no. 11, 1984.

[8] T. Flash and N. Hogan, "The coordination of arm movements: An experimentally confirmed mathematical model," *The Journal of Neuroscience*, vol. 5, no. 7, 1985.

[9] G. J. Garvin, M. Žefran, E. A. Henis, and V. Kumar, "Two-arm trajectory planning in a manipulation task." Submitted to Biological Cybernetics, 1995.

[10] Y. Uno, M. Kawato, and R. Suzuki, "Formation and control of optimal trajectory in human multijoint arm movement," *Biological Cybernetics*, vol. 61, 1989.

[11] M. Kawato, "A bi-directional theory approach to prerational intelligence," in *Proceedings of ZiF Conference on Prerational Intelligence*, (Bielefeld, Germany), 1994.

[12] M. Žefran and V. Kumar, "Optimal control of systems with unilateral constraints," in *Proc. of 1995 IEEE Int. Conf. on Robotics and Automation*, (Nagoya, Japan), 1995.

[13] J. Gregory and C. Lin, *Constrained optimization in the calculus of variations and optimal control theory.* New York: Van Nostrand Reinhold, 1992.

[14] G. Garvin, "Trajectory formulation in human movement: An extension of existing models for single arm motions to coupled motions of two arms." Master Thesis, University of Pennsylvania.

[15] D. A. Winter, *Biomechanics and motor control of human movement.* New York: John Wiley & Sons, second ed., 1990.